GEOLOGICAL FRACTURE MAPPING USING ELECTROMAGNETIC GEOTOMOGRAPHY

A.L. Ramirez, F.J. Deadrick and R.J. Lytle

Lawrence Livermore National Laboratory
Livermore, California 94550

ABSTRACT

This article describes the evaluation of a new geophysical technique used to map fractures between boreholes: electromagnetic geotomography used in conjunction with salt water tracers. An experiment has been performed in a granitic rock mass. Geotomographic images have been generated and compared with borehole geophysical data: neutron logs, acoustic velocity logs, caliper logs and acoustic televiewer records. Comparisons between the images and the geophysical logs indicate that clusters of fractures were detected but single fractures were not.

INTRODUCTION

The mapping of fractures within a rock mass is a three dimensional problem. It requires that fractures be detected and measured along exposed surfaces such as boreholes or tunnel walls. In many instances, this information can be successfully projected into the rock mass for short distances. However, as the projection distance increases, the uncertainty associated with the projections becomes larger and may become unacceptable.

There are borehole geophysical methods which offer a high level of resolution when used to detect fractures (e.g., acoustic televiewer). These methods, however, cannot penetrate deeply into the rock mass. Other methods (e.g., cross-borehole seismic) can probe deep into the rock and may provide evidence that fractures

exist but they lack the resolution necessary to map these fractures. Consequently, the Panel on Rock Mechanics Research Requirements (1981) has recommended that improvements be achieved in methods used to map fractures remotely (between boreholes).

GEOTOMOGRAPHY METHOD

Electromagnetic geotomography was combined with the use of salt water tracers to map fractures remotely. Geotomography was developed at LLNL and has been thoroughly described elsewhere (Lytle et al., 1978, Lytle et al., 1981). In this section we describe important characteristics of the geotomography method.

The geotomography method is a new way of collecting and interpreting geophysical data. The method is similar in concept to the data collection and interpretation procedures used in medical diagnostics, such as brain and body scans. Figure 1 shows how the geotomography method is used to collect subsurface geophysical data. By varying the depths of the transmitter and receiver in two boreholes, it is possible to detect regions having different properties using either electromagnetic waves or seismic waves. Multiple ray paths propagated along many different orientations are used to provide many different "views" of a region.

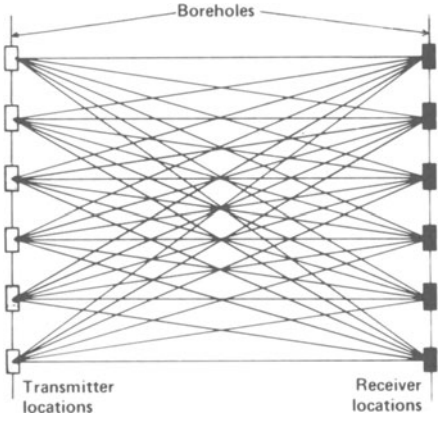

Fig. 1. Method used to sample the rock mass. The antennas are moved along the boreholes to provide many different perspectives of the rock between boreholes.

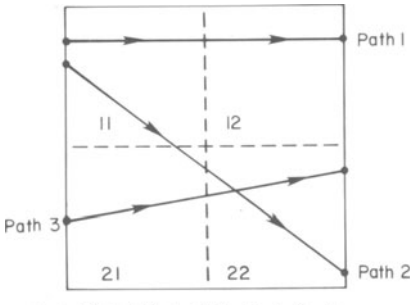

$$X_1 = {}_1D_{11}\alpha_{11} + {}_1D_{12}\alpha_{12} + {}_1D_{21}\alpha_{21} + {}_1D_{22}\alpha_{22}$$

$$X_2 = {}_2D_{11}\alpha_{11} + {}_2D_{12}\alpha_{12} + {}_2D_{21}\alpha_{21} + {}_2D_{22}\alpha_{22}$$

$$X_3 = {}_3D_{11}\alpha_{11} + {}_3D_{12}\alpha_{12} + {}_3D_{21}\alpha_{21} + {}_3D_{22}\alpha_{22}$$

Fig. 2. Example of the method used to interpret the electromagnetic attenuation measurements.

The geophysical data is interpreted using a modified version of the back projection technique described by Kuhl and Edwards (1968). As a first step, the area between two boreholes is divided into a set of cells (i.e., smaller zones) by arbitrarily spaced vertical and horizontal lines. The objective is to infer the electromagnetic attenuation factor induced by the rock and the fluid-filled fractures within each of these. The attenuation factor is defined as α if the amplitude of a plane wave is reduced by the factor exp $(-\alpha x)$ in traveling a distance of x meters (Sheriff, 1973). The resulting image will be a map showing the variations of the electromagnetic factor throughout all the cells. Fracture zones can be mapped on this image because they will appear as zones which create larger attenuation factors than those of intact rock. We use gray scale images to present the results of these calculations. In a gray scale image, a tone of gray is assigned to each cell. This tone represents the attenuation factor calculated for that cell.

Figure 2 shows a simplified example of the algorithm used to calculate the attenuation factor for each cell. For this example, the region between two boreholes was arbitrarily divided into four cells, and only three ray paths were used to sample the region. (For an actual geotomograph, many more cells and ray paths are used.) The attenuation X of rays, 1, 2, and 3 is expressed mathematically in Fig. 2: α_{11}, α_{12}, α_{21}, and α_{22} represent the attenuation factors characteristic of cells 11, 12, 21, and 22 respectively, and D_{11}, D_{12}, D_{21}, and D_{22} represent the distances which each ray path covered through these cells. Similar equations are constructed for ray paths 2 and 3 This set of linear equations is then solved iteratively for α_{11}, α_{12}, α_{21}, and α_{22}.

EXPERIMENT DESCRIPTION

An experiment has been performed at a site near the town of Oracle, Arizona, approximately 64 km north of the city of Tucson. The electromagnetic geotomography method was used in combination with salt water tracers which were forced into the granitic rock mass present at the site. The experimental site has been developed by the University of Arizona for the U.S. Nuclear Regulatory Commission. The granite rock mass contains an extensive network of fractures. These are quite numerous and exhibit large variability in orientation.

Figure 3 shows the four roughly coplanar boreholes available at the site during the experiment. Also shown are the various measurement zones for which geotomographic images have been constructed.

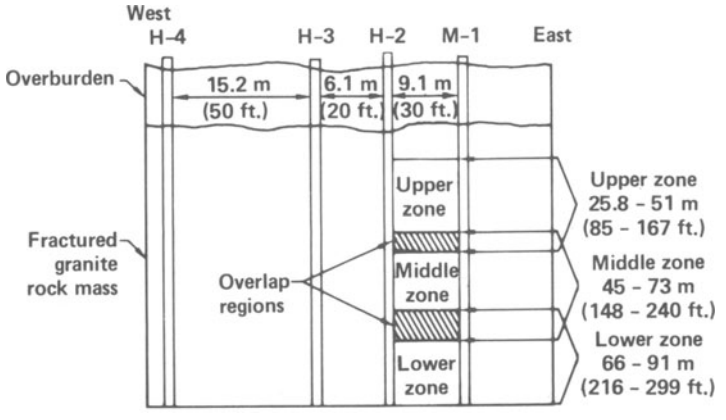

Fig. 3. Cross section of the experimental site showing the different rock mass regions probed between boreholes M-1 and H-2.

Measurements of the attenuation of electromagnetic waves were obtained in the field before and after the salt water was forced into the fracture network. We forced the salt water into the fractures by filling the full length of borehole M-1 with salt water while lowering the water level in borehole H-3 with a submersible pump. The salt water used had a conductivity ten times greater than that of the natural groundwater.

EXPERIMENTAL RESULTS

Geotomographs have been generated for all the measurement zones shown in Fig 3. It has been assumed that boreholes M-1 and H-2 are vertical. Examples of these will be shown below; the remaining images are presented and analyzed by Ramirez et al., (1982).

Figure 4 shows a comparison of the lower measurement zone geotomograph (refer to Fig. 2) and geophysical logs of boreholes M-1 and H-2. The logs were recorded by W. Scott Keys of the U.S. Geological Survey. The right margin of the image coincides with borehole M-1 whereas the left margin coincides with borehole H-2. Zones of probable fracturing along the borehole wall are indicated by deflections in the logs.

Fractures should be indicated on the acoustic velocity and neutron logs by deflections to the left. On the caliper logs, most fractures should correspond with deflections to the right. The raw data for the geotomographic image was collected two days

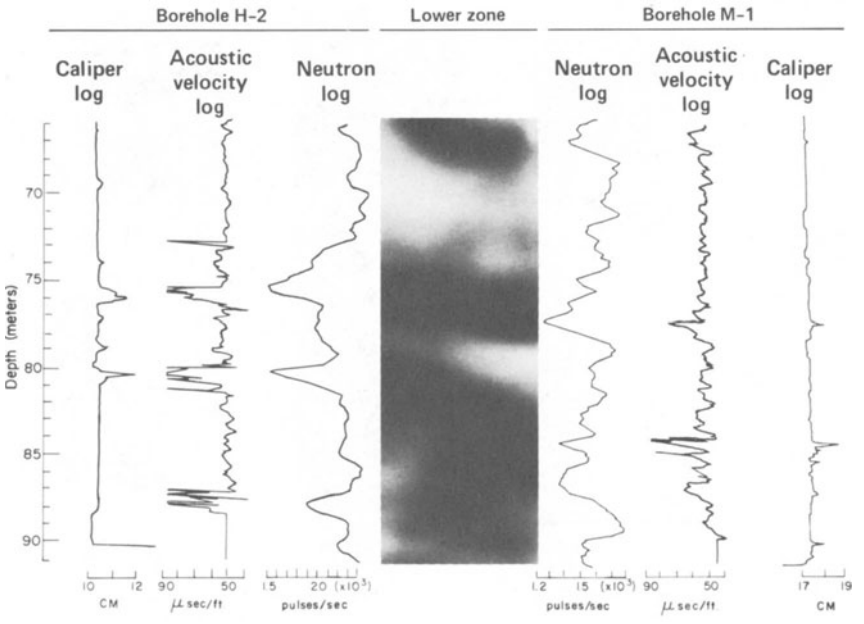

Fig. 4. Comparison of M-1 and H-2 geophysical logs with the lower measurement zone geotomograph. The data for this image was obtained after salt water was forced into the rock mass.

after salt water was introduced into borehole M-1.

This figure shows the most prominent correlations observed between the single borehole geophysical logs and the cross-borehole geotomographs. The darker colors in the image show the rock mass zones which caused the largest attenuation of the signal; hence, fractured zones should be represented by the darker colors. Good agreement is shown between logs and images from zones of inferred fracturing. The anomaly visible near the middle of the image at a depth of 76.5 m (251 ft) was tentatively identified by the U.S. Geological Survey as one of the most permeable and pervasive features identified on the geophysical logs (Keys, 1981).

Figure 5 shows a comparison of three geotomographs corresponding to the upper measurement zone. The center image shows the same region after salt water was forced into the rock. The image to the right is a difference geotomograph obtained by subtracting the "before" (left) image from the "after" (central) image. Note that the right hand image is substantially different from the other two. It shows the changes in electromagnetic attenuation factor created by the intrusion of salt water. The darker colors represent zones where maximum changes occurred.

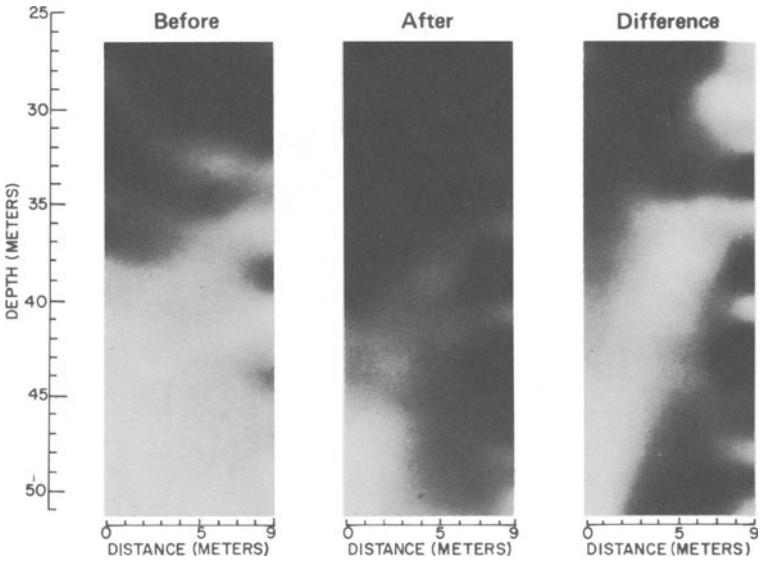

Fig. 5. Geotomographs of the upper measurement zone before and after salt water tracers were forced into the rock mass. A third geotomograph obtained by subtracting the "before" from the "after" is also shown.

Difference geotomographs appear to provide some advantages. These will highlight zones where signal attenuation is small but the change in attenuation is high. For example, a physically small permeable zone may induce small signal losses which may be difficult to detect on a standard geotomographic image. However, when a difference geotomograph is constructed, those fractures will be highlighted because the change in electromagnetic attenuation created by the intrusion of salt water can be relatively high. An example of this may be observed at a depth of 48.5 meters in Fig. 5.

FACTORS RELEVANT TO THE SUCCESSFUL APPLICATION OF THE METHOD

The electromagnetic geotomography method can be used to map the subsurface under certain conditions. Boreholes which penetrate and straddle the area of interest need to be available. They should be uncased or have casing made of nonconductive casing materials, such as plastic. Otherwise the electromagnetic energy will travel up and down the casing only and will not penetrate the rock mass.

The minimum distance between the transmitter and receiver antennas should be much greater than $\lambda/2\pi$ (where λ is the wavelength of the waves in the rock mass). If this condition is met,

the dominating electrical fields detected by the receiver antenna will attenuate linearly with distance and linear equations can be used in the reconstruction algorithms. Fortunately, the wave frequencies generally appropriate for probing have relatively small wavelengths, so the requirement is easily satisfied. For example, in Oracle $\lambda/2\pi$ was approximately 0.5 m when 40 MHz waves were used.

The probing geometry will control the resolution which can be achieved with geotomography. It will be defined by the locations of the transmitting and receiving antennas; in most applications, the total depths and alignments of the boreholes will determine the antennas' positions. Maximum resolution will be achieved when the area of interest can be totally encircled by the antennas. In most applications it will not be practical to do so but acceptable alternatives can be followed. At Oracle, for example, the antennas were moved along lines which extended far above and below the center of the measurement zone. In this manner, the antennas effectively rotated roughly 300 degrees around the center of the measurement area.

The geological features to be mapped using electromagnetic geotomography should have electrical properties different from those of the surrounding rock mass. Fractures filled with water offer good contrast relative to the surrounding rock when the rock itself contains little or no water within its pores and most of the water storage in the rock mass is along the fracture planes. These conditions are met by low porosity rocks, such as igneous rocks, which exist below the water table. Rocks such as sand- stones or claystones, which store significant amounts of water in their pores, will be less desirable candidate media because the contrast between intact rock and fracture planes will be significantly smaller.

SUMMARY AND CONCLUSIONS

The potential of the electromagnetic geotomography method to map fractures remotely has been evaluated. A fractured granitic rock mass has been investigated and geotomographic images of the rock mass have been generated. These images were compared with borehole geophysical data (neutron logs, acoustic velocity logs, caliper logs, and acoustic televiewer records) and analyzed.

Comparisons between the geotomographic images and the borehole geophysical data suggest that geotomography has merit when used to map fractures in granite. In general, image anomalies coincide with geophysical log anomalies which can be indicative of fracturing along the borehole walls. Given the experimental conditions of the Oracle experiment, available data suggests that clusters of fractures (i.e., fracture zones) were detected but single fractures were not.

The results from Oracle indicate that salt water tracers create changes in electromagnetic attenuation which are useful to detect fractured zones filled with tracers. The contrast is artificially increased between fractures which accept the salt water and the intact rock. When salt water tracers are used and data is collected before and after tracers penetrate the fractures, a difference geotomographic image can be obtained. It appears to reveal smaller fractured zones, otherwise unrecognizable, which salt water has penetrated. A difference image will also tend to eliminate geological features which attenuate the electromagnetic signal but are not permeable fractures.

The conclusions presented herein should be considered tentative. They hinge upon the correlations of the geotomographic images and geophysical logs. The borehole geophysical methods only sample the rock mass along the borehole walls whereas the geotomography method samples the rock mass between the boreholes. These correlations are limited by the degree to which we can extrapolate the information provided by the geophysical logs into the rock mass between the boreholes. Exploratory boreholes will be drilled to verify the information provided by images.

ACKNOWLEDGMENTS

This work was funded by the U.S. Nuclear Regulatory Commission, Office of Nuclear Regulatory Research.

"Work performed under the auspices of the U.S. Department of Energy by the Lawrence Livermore National Laboratory under Contract number W-7405-ENG-48."

REFERENCES

1. W.S. Keys, 1981, Private Communication, Technical Memorandum No. 69, U.S. Geological Survey, Denver, Colorado.
2. D.E. Kuhl and R.Q. Edwards, 1968, "Reorganizing Data from Transverse Scans of the Brain Using Digital Processing," Radiology, Vol. 91, No. 5.
3. R.J. Lytle, L.A. Dines, E.F. Laine and D.L. Lager, 1978, "Electromagnetic Cross-Borehole Survey of a Site Proposed for an Urban Transit Station," UCRL-52484, Lawrence Livermore National Laboratory, Livermore, California.
4. R.J. Lytle, D.L. Lager, E.F. Laine, J.D. Salisbury and J.T. Okada, 1981, "Fluid-Flow Monitoring Using Electromagnetic Probing," Geophysical Prospecting, Vol. 29, pp. 627-638.
5. Panel on Rock Mechanics Research Requirements, 1981, "Rock Mechanics Research Requirements for Resource Recovery, Construction, and Earthquake-Hazard Reduction," U.S. National Committee for Rock Mechanics, National Research Council, National Academy Press.

6. A.L. Ramirez, F.J. Deadrick and R.J. Lytle, 1982, "Cross-Borehole Fracture Mapping Using Electromagnetic Geotomography," UCRL-53255 (in preparation), Lawrence Livermore National Laboratory, Livermore, California.
7. R.E. Sheriff, 1973, The Encyclopedic Dictionary of Exploration Geophysicists, Society of Exploration Geophysicists, Tulsa.